

Worsened Punch Sticking by External Lubrication with Magnesium Stearate

Tianyi Xiang and Changquan Calvin Sun*

Pharmaceutical Materials Science and Engineering Laboratory, Department of Pharmaceutics,

College of Pharmacy, University of Minnesota, Minneapolis, MN 55455, United States

**Corresponding author*

Changquan Calvin Sun, Ph. D.

9-127B Weaver-Densford Hall

308 Harvard Street S.E.

Minneapolis, MN 55455

Email: sunx0053@umn.edu

Tel: (612) 624-3722

Fax: (612) 626-2125

1 **Abstract**

2
3 External lubrication of tooling with magnesium stearate (MgSt) is a common strategy to eliminate
4 punch sticking when compressing powders with a high sticking propensity, such as many pure
5 active pharmaceutical ingredients (APIs). We found that it actually led to aggravated punch
6 sticking at low compaction pressures. This counterintuitive phenomenon was explained based on
7 interplay of forces among the punch tip, MgSt, and API. The explanation is supported by the
8 observed effects of pressure and mechanical properties of APIs on this phenomenon.

91. Introduction

10

11 The tablet has been widely used in drug delivery due to its physical and chemical stability,
12 low manufacturing cost, and good patient compliance (Kottke and Rudnic, 2002; Sun, 2017). A
13 common problem during tablet manufacturing is punch sticking, which may be defined as the
14 adherence of the powder material onto the tooling surface during powder compaction (Paul et al.,
15 2017a). If not eliminated, punch sticking leads to tablet defects, low manufacturing efficiency,
16 and even loss of batches (Chattoraj et al., 2018). Punch sticking occurs when the total force of an
17 API particle bonding with the punch surface (F_1) is higher than that between the API particle and
18 neighboring particles in tablet (Paul et al., 2017a). With repeated compression, the severity of
19 API sticking to the punch depends on the force between API particles adhered to punch and API
20 particles in a new tablet (F_2) relative to the force between the API particles in a new tablet and
21 neighboring excipient particles (F_3). After repeated compression, a monolayer is formed when F_2
22 $< F_3$, or multiple layers form when $F_2 > F_3$ (Paul et al., 2017a). Furthermore, the kinetics of
23 punch sticking can be described by the Hill's equation (Paul et al., 2017a).

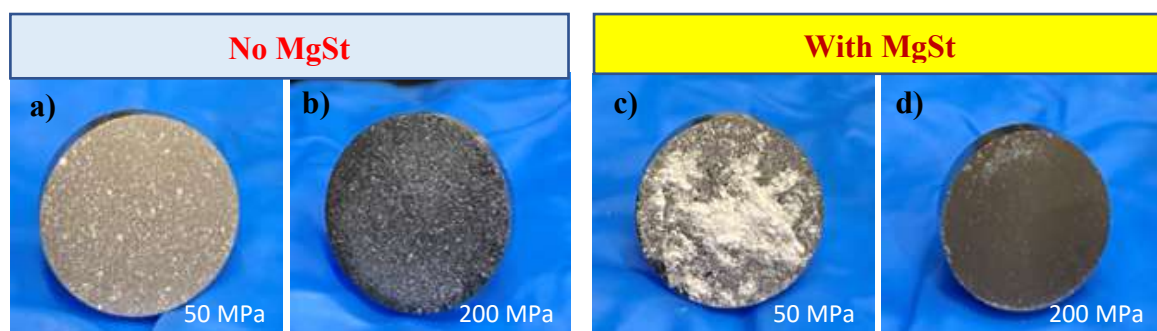
24 Strategies used to mitigate or eliminate punch sticking problems can be broadly divided
25 into three categories: 1) API crystal and particle engineering, such as salt and cocrystal formation
26 (Al-Karawi and Leopold, 2018; Paul et al., 2019; Wang et al., 2020), particle size and morphology
27 modification (Capece, 2019; Wagnis et al., 2014; Hooper et al., 2017; Paul et al., 2020; Chen et
28 al., 2020), and containment of API in a porous carrier (Paul et al., 2023); 2) modification of process
29 parameters, such as compaction pressure (Paul et al., 2017b; Al-Karawi et al., 2017; Capece, 2019;
30 Billany and Richards, 1982; Mitrove and Augsburger, 1980; Danjo et al., 1997; Kakimi et al., 2010;
31 Roberts et al., 2003; Roberts et al., 2004; Swaminathan et al., 2017; Waimer et al., 1999; Wang et
32 al., 2015; Wang et al., 2004) and tooling design (Waimer et al., 1999; Roberts et al., 2004; Roberts
33 et al., 2003); 3) formulation design, such as using different excipients (Abdel-Hamid and Betz,
34 2012; Badal Tejedor et al., 2015; Paul and Sun, 2018), reducing API loading (Hutchins et al.,
35 2012; Capece, 2019), and changing lubricant level in tablet formulation (Gunawardana et al., 2023;
36 Capece, 2019; Al-Karawi et al., 2017; Badal Tejedor et al., 2015; Roberts et al., 2004;
37 Swaminathan et al., 2017; Billany and Richards, 1982; Mitrove and Augsburger, 1980; Patel and
38 Dave, 2021).

39

40 It is known that mixing a powder with MgSt, i.e., internal lubrication, can significantly
41 change tableting behaviors of some powders (Dun et al., 2020; He et al., 2007) and may lead to
42 higher tablet friability and slower tablet dissolution performance (Paul and Sun, 2017; Li-Hua and
43 Chowhan, 1990; Uzunović and Vranić, 2007; Billany and Richards, 1982). Given these known
44 issues with internal lubrication, external lubrication has been pursued to reduce ejection force and
45 punch sticking problem in commercial tablet manufacturing (de Backere et al., 2023). Compaction
46 properties of pure APIs can offer invaluable insights into tablet formulation design, such as
47 excipient selection. In such studies, it is common to lubricate tablet tooling with magnesium
48 stearate (MgSt) before compression to avoid punch sticking (Jahn and Steffens, 2005).

49 However, we surprisingly observed that tablet tooling lubricated with MgSt sometimes
50 worsened punch sticking during compression. For example, sodium cyclamate exhibited slight
51 punch sticking after compression at both 50 MPa and 200 MPa when clean punches were used
52 (Figure 1a, b). After coating the punch tip with a layer of MgSt, sticking was much more severe at
53 50 MPa compaction pressure (Figure 1c). However, punch sticking was absent at 200 MPa
54 compaction pressure (Figure 1d). This unexpected deterioration of punch-sticking performance
55 by external lubrication of tooling with MgSt and the effect of pressure cannot be explained by the
56 existing **punch sticking** model, which was developed to explain **behaviors** of formulated API
57 during compaction using a clean punch (Paul et al., 2017a). Hence, we propose a new punch-
58 sticking model to explain this surprising phenomenon.

59



60
61 **Figure 1.** The sticking behaviors of sodium cyclamate under different compaction conditions; a)
62 no MgSt, 50 MPa; b) no MgSt, 200 MPa); c) with MgSt (50 MPa); d) with MgSt (200 MPa)

63

64 **2. A Punch Sticking Model for External Lubrication**

65

66 The new punch sticking model for the scenario of external lubrication differs from the
67 previous punch sticking model in two aspects: 1) punches used for compression, instead of being
68 clean, are coated with a layer of MgSt, and 2) API is not mixed with an excipient. Consequently,
69 whether or not sticking occurs depends on the interplay among a different set of forces, i.e., 1) the
70 force between punch tip and MgSt (F_{pm}); 2) the force between MgSt and API (F_{ma}); and 3) the
71 force between API and API (F_{aa}). In this new model, punch sticking takes place when F_{pm} and
72 $F_{ma} > F_{aa}$, but is absent when $F_{pm} < F_{ma}$ and F_{aa} . It should be mentioned that the total force between
73 any pair of particles depends on the effective bonding area (BA) and bonding strength (BS) (Osei-
74 Yeboah et al., 2016). A larger BA or BS or both favors a higher total bonding force between two
75 particles. While BS depends on chemical nature and surface energy of the particles, BA depends
76 on compaction pressure, particle size, and hardness of the particles in contact (Sun, 2011).

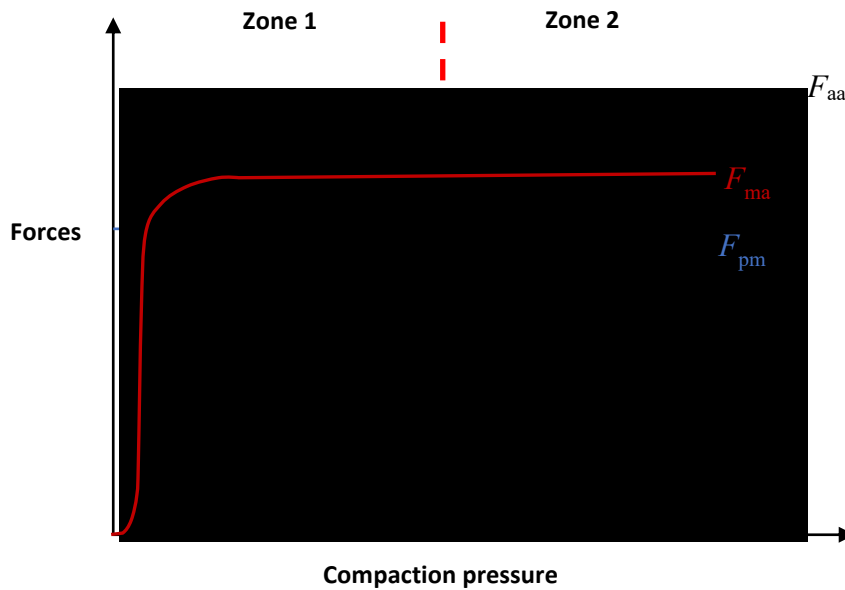
77

78 There are a few important features of this model that are worth mentioning. First, the punch
79 tip is covered by a continuous layer of MgSt prior to compression, i.e., the contact area between
80 MgSt and punch is at the maximum. Consequently, F_{pm} would be independent of pressure for a
81 given set of tooling and a batch of MgSt (Figure 2). In contrast, both F_{ma} and F_{aa} are pressure-
82 dependent since BA usually increases with increasing compaction pressure due to more extensive
83 plastic deformation till a maximum value is reached. Second, MgSt is a soft material (Sun, 2015),
84 likely softer than most API particles. If so, API particles in contact with the MgSt layer penetrate
85 into it during compression, leading to a sharper rise in BA between MgSt and API than that
86 between API particles (Figure 2). For an API that is significantly harder than MgSt, a negligible
87 BA between the first and second layers of API is developed when the maximum BA between MgSt
88 and API has been attained. BA of API-API can also reach a maximum, but only at significantly
89 higher pressures. The different BA growth profiles with increasing pressure lead to F_{ma} rising
90 more quickly to a plateau than F_{aa} (Figure 2).

91

92 The curvatures of F_{aa} and F_{ma} are expected to be S-shaped, which is analogous of the full
93 tableability profiles of powders (Vreeman and Sun, 2022, Chang and Sun, 2020). Therefore, the
94 condition of F_{pm} and F_{ma} are both greater than F_{aa} (F_{pm} and $F_{ma} > F_{aa}$) will be satisfied in a low-
95 pressure range, leading to punch sticking (zone 1 in Figure 2). At high pressures, no sticking is

96 observed because MgSt is peeled off the punch surface when the condition of F_{pm} is lower than
97 F_{ma} and F_{aa} (i.e., $F_{pm} < F_{ma}$ and F_{aa}) is met (zone 2 in Figure 2).



98
99 **Figure 2.** The conceptual profiles of F_{aa} , F_{ma} , and F_{pm} varying with compaction pressure. In zone
100 1, sticking is evident. In zone 2, sticking is avoided because MgSt is detached from punch surface
101 when F_{aa} and F_{ma} are both higher than F_{pm} .

102
103 **3. Materials and Methods**

104
105 **3.1 Materials**

106 Ibuprofen (IBU; Sigma Aldrich, St. Louis, MO), celecoxib (CEL; Aarti Drugs Pvt Ltd.,
107 Mumbai, India), magnesium stearate (MgSt; non-bovine, HyQual™, Mallinckrodt, St. Louis, MO),
108 sodium cyclamate (CycNa; Acros Organics®, Geel, Belgium), and acetaminophen (ACM, Form
109 I) (Sigma Aldrich, St Louis, MO) were all used as received.

110
111 **3.2. Methods**

112 **3.2.1. Powder compaction**

113 Compaction of powders was conducted on a compaction simulator (Styl'One Evolution;
114 MedelPharm, Beynost, France) using a force-controlled, symmetrical single compression cycle (2%
115 speed, 2 s compression composed of a 1 s rise and a 1 s fall without holding at the maximum force,

116 followed by 3 s relaxation, and a 2 s ejection step). A 12.7 mm round flat tooling (B type) with a
117 removable upper punch tip was used for all the compaction and sticking assessment. A suspension
118 of MgSt in ethanol (10%, w/v) was applied onto the punch surface with a brush and air-dried
119 before compaction. Depending on the material, different compaction pressures (4 - 400 MPa) were
120 used. At each pressure, 5 tablets were compressed following an identical procedure. The punch tip
121 was cleaned and coated with a visually uniform layer of MgSt before each compression.

122

123 **3.2.2. True density**

124 The true density (ρ_t) of IBU, CEL, CycNa, ACM, and MgSt was determined using a helium
125 pycnometer (Quantachrome Instruments, Ultrapycnometer 1000e, Byonton Beach, Florida) with
126 1–2 g of an accurately weighed sample that filled about 75% of the volume of the sample cell. An
127 analytical balance (Mettler Toledo, Columbus, Ohio, model AG204) was used for weighing. The
128 experiment was stopped when the variation between five consecutive measurements was below
129 0.005% and the mean of the last five measurements was calculated, which was taken as the true
130 density.

131

132 **3.2.3. In-die Heckel analysis**

133 In-die tablet porosity (ε) data was calculated from in-die tablet thickness measured with
134 the compaction simulator, ρ_t , and the weight of the ejected tablet. In-die mean yield pressure ($P_{y,i}$)
135 was obtained from a linear regression of the linear portion of the $-\ln(\varepsilon)$ vs. P profile, i.e., the
136 Heckel plot, according to Eq. (1). (Heckel, 1961a, 1961b)

$$137 \quad -\ln(\varepsilon) = \frac{1}{P_{y,i}} P + A \quad (1)$$

138

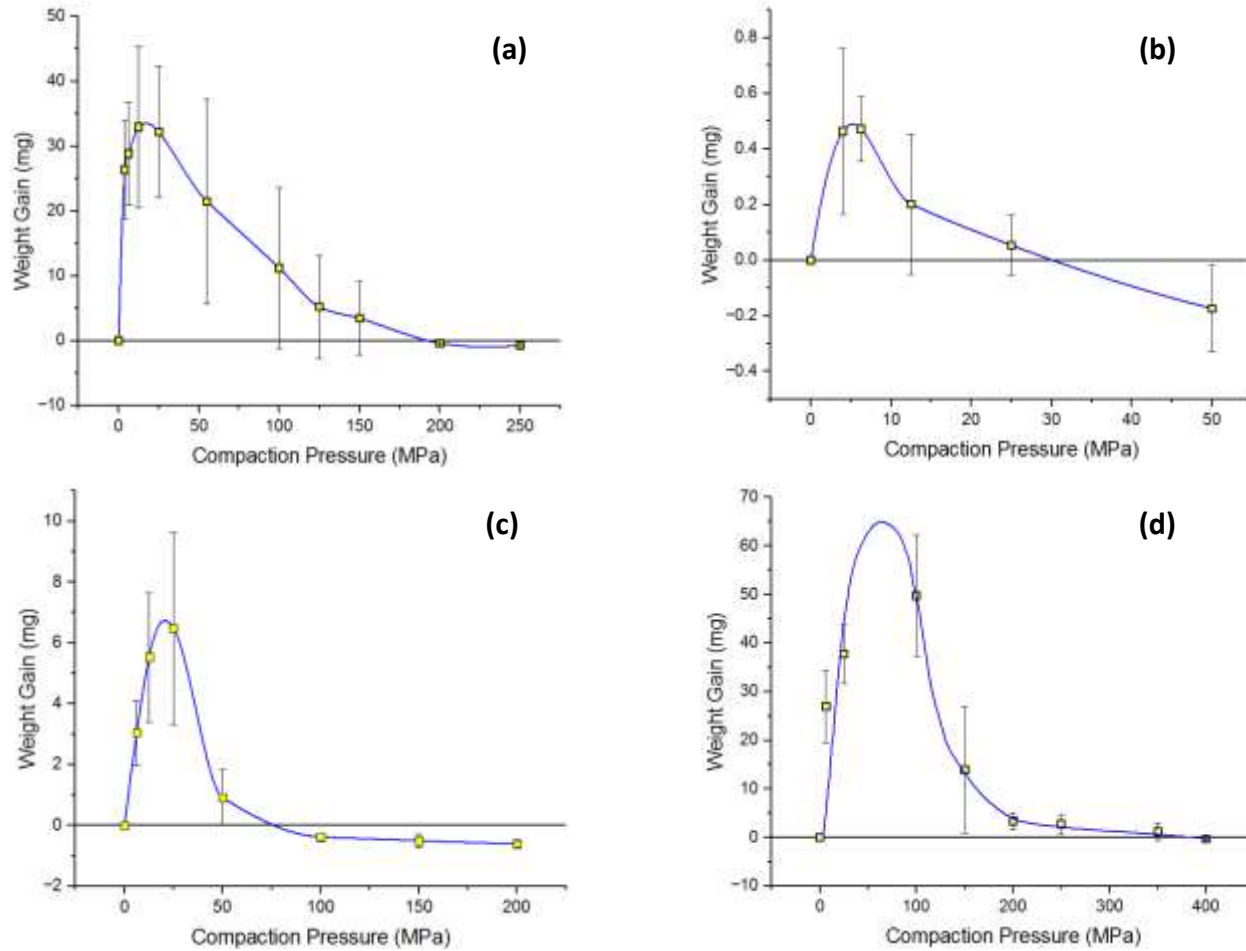
139 **3.2.4. Assessment of sticking behavior by weight gains**

140 Punch sticking was quantified by the weight gain of the removable upper punch tip after
141 each tablet was compressed. The various weights of the removable upper punch tip, i.e., clean tip
142 (W0), tip with MgSt coating (W1), and tip after compression (W2), were recorded. The weight of
143 the MgSt layer (W1-W0) and the weight gain after compression (W2-W1) were calculated. A
144 positive weight gain indicates sticking of API onto the punch tip, while a negative weight gain
145 indicates peeling-off of the MgSt from the punch tip.

146

147 **4. Results and Discussion**

148 Although the extent of punch sticking varied among the four model APIs, i.e., IBU, CEL,
149 CycNa, and ACM, they all showed a qualitatively similar pattern in their weight gain profiles
150 (Figure 3). With increasing compaction pressure, the weight gain initially increases, then decreases,
151 and eventually becomes negative.



152

153

154 **Figure 3.** The plots of weight gain of punch tip after compression versus compaction pressure for
155 a) sodium cyclamate (CycNa), b) acetaminophen (ACM); c) celecoxib (CEL); and d) ibuprofen
156 (IBU).

157

158 This common shape of these plots is consistent with the observation that punch sticking
159 was severe at low pressures (Figure 1c) but eliminated at high pressures (Figure 1d). The positive
160 weight gain at low pressures suggests that the condition of F_{pm} and $F_{ma} > F_{aa}$ has been met, while

161 the negative weight gain (an absence of punch sticking) at high pressures suggests that the
162 condition of $F_{\text{pm}} < F_{\text{ma}}$ and F_{aa} has been met.

163

164 The validity of the model depends on the assumption that MgSt is softer than an API. This
165 assumption is supported based on their $P_{y,i}$ values (Table 1), which suggests the plasticity follows
166 the descending order of MgSt > IBU \geq CEL > ACM > CycNa. Under this condition, the pressure-
167 depending sticking behaviors can be explained by considering the pressure dependence of BA and,
168 hence, total bonding force between different pairs (F_{pm} , F_{ma} , and F_{aa}), as explained below.

169

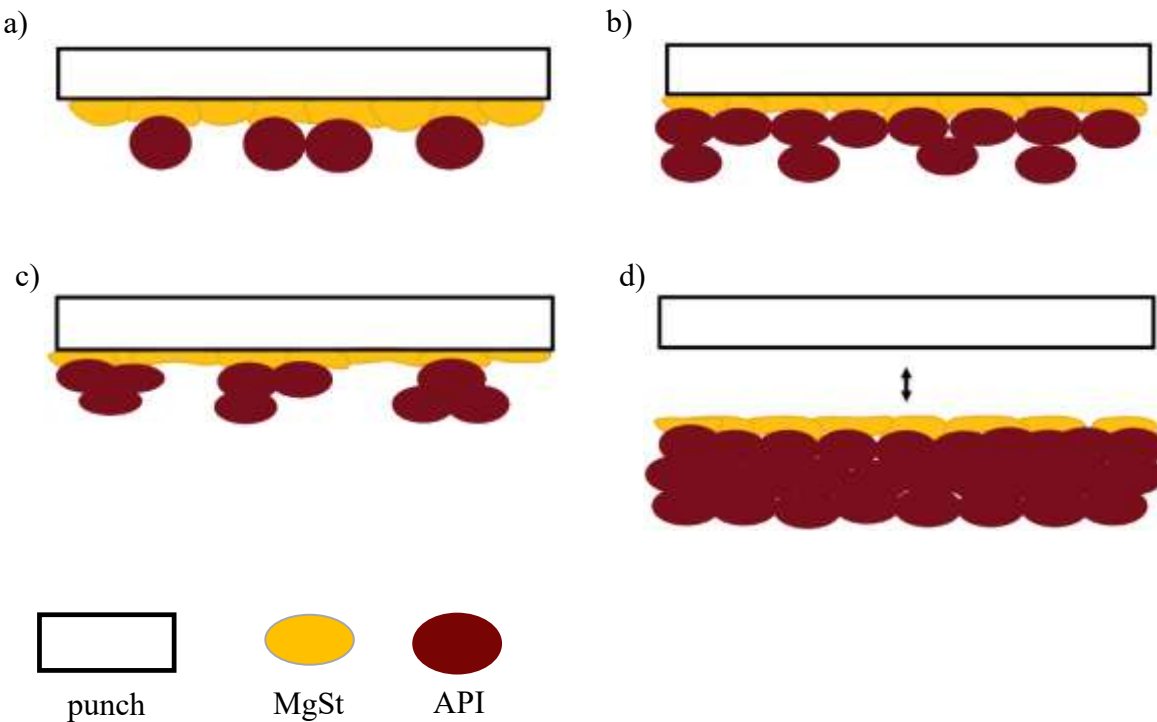
170 **Table 1.** In-die $P_{y,i}$ values of APIs and MgSt (n = 3).

Materials	In-die P_y (MPa)
Magnesium stearate	25.8 \pm 4.5
Ibuprofen	40.5 \pm 9.9
Celecoxib	47.1 \pm 8.3
Acetaminophen	89.5 \pm 2.7
Sodium cyclamate	108.3 \pm 4.7

171

172 In the very low-pressure range (Figure 4a), MgSt particles deform much more than API
173 particles due to the significantly higher plasticity of MgSt than API. Thus, the BA between MgSt
174 and API is much larger than that between API particles. Note that the bonding force between
175 MgSt and punch already reached the maximum at the beginning because of the MgSt layer was
176 applied through drying a suspension of MgSt. As a result, F_{pm} and $F_{\text{ma}} > F_{\text{aa}}$ (Figure 4a) and
177 sticking occurs. With increasing pressure, the BA between MgSt and API particles grows rapidly
178 while that between API particles does not change much. Hence, the condition of F_{pm} and $F_{\text{ma}} >$
179 F_{aa} is still satisfied to assure sticking despite the changes in BA. However, since more API
180 particles can encounter the MgSt layer at a higher pressure, the amount of API transferred to punch
181 tip grows (Figure 4b). When the pressure further increases, the BA between MgSt and API
182 particles starts to saturate, but the BA between API particles continues to increase. As some point,
183 some of the API particles are removed from the MgSt layer when F_{aa} surpasses F_{ma} , leading to a

184 decrease in the amount of API stuck onto the punch tip (Figure 4c). When the compaction pressure
185 is sufficiently high, both MgSt and API particles undergo extensive plastic deformation, leading
186 to maximum BA of MgSt-API and API-API, and the condition of $F_{pm} < F_{ma}$ and F_{aa} is met so that
187 the MgSt layer is peeled off from the punch tip (Figure 4d), leading to a negative weight change.



188
189 **Figure 4.** Evolution of bonding interactions among different particles as a function of compaction
190 pressure. a) low pressure (positive weight gain due to API particles sticking to the MgSt layer); b)
191 medium pressure (peak value of weight gain profiles), c) medium – high pressure (reduced weight
192 gain), d) high pressure (negative weight gain corresponding to the peeling off of MgSt from punch)
193

194 The peak value of weight gain varied widely with API, from 0.5 – 50 mg, which is dictated
195 by the size, density, and number of layers of API particles adhered to the punch. Given the
196 complexity of this phenomenon and variability in weight gain, quantitative description of the
197 maximal weight gain or the shape of the profiles cannot be predicted in this work. However, we
198 note that the high peak values of weight gain profiles of IBU, CycNa, and CEL, are accompanied
199 by capping or lamination of tablets upon ejection. Consequently, multiple layers of API particles
200 were transferred onto the punch tip, leading to higher peak weight gains. The average of the

201 maximum negative weight gain varied in a narrow range of 0.17 – 0.68 mg for the four APIs,
202 roughly corresponding to the amount of MgSt coated onto punch tip (0.36 – 1.24 mg).

203

204 **Lastly**, this new punch-sticking model predicts that an API that is softer than MgSt may not
205 exhibit punch sticking even at low pressures, if the BS between API particles is similar or higher
206 than that **between MgSt and API**. However, we could not identify an API that is softer than MgSt
207 to further test the model in this way.

208

209 5. Conclusions

210 The counterintuitive observation of a MgSt coating layer worsening punch-sticking of API
211 at low pressures is explained using a model that considers the interplay among F_{pm} , F_{ma} , and F_{aa}
212 as a function of pressure. This model predicts severe punch sticking at low pressures but an
213 absence of punch sticking at sufficiently high pressures. Results from this investigation using four
214 API powders support the proposed model. **They suggest that increasing pressure is likely an**
215 **effective approach to overcome punch sticking problems, if observed during tablet manufacturing**
216 **when external lubrication is used.** This work **also** affirms the validity of the approach to predict
217 punch sticking behavior based on interaction forces between different pairs of materials, i.e., punch,
218 API, and excipient (magnesium stearate in this work). Thus, it not only explains an intriguing
219 phenomenon, but also offers a general approach for a fundamental understanding of the complex
220 phenomenon of punch sticking **in other scenarios** during tablet manufacturing.

221

222 ACKNOWLEDGMENT

223 CCS thanks the National Science Foundation for support through the Industry University
224 Collaborative Research Center (IUCRC) grant IIP-2137264, Center for Integrated Materials
225 Science and Engineering for Pharmaceutical Products (CIMSEPP).

References

Abdel-Hamid, S., Betz, G., 2012. A novel tool for the prediction of tablet sticking during high speed compaction. *Pharm. Dev. Technol.* 17, 747–754. <https://doi.org/10.3109/10837450.2011.580761>

Al-Karawi, C., Leopold, C.S., 2018. A comparative study on the sticking tendency of ibuprofen and ibuprofen sodium dihydrate to differently coated tablet punches. *Eur. J. Pharm. Biopharm.* 128, 107–118. <https://doi.org/10.1016/j.ejpb.2018.04.004>

Al-Karawi, C., Lukášová, I., Sakmann, A., Leopold, C.S., 2017. Novel aspects on the direct compaction of ibuprofen with special focus on sticking. *Powder Technol.* 317, 370–380.

Badal Tejedor, M., Nordgren, N., Schuleit, M., Rutland, M.W., Millqvist-Fureby, A., 2015. Tablet mechanics depend on nano and micro scale adhesion, lubrication and structure. *Int. J. Pharm.* 486, 315–323. <https://doi.org/10.1016/j.ijpharm.2015.03.049>

Billany, M., Richards, J., 1982. Batch variation of magnesium stearate and its effect on the dissolution rate of salicylic acid from solid dosage forms. *Drug Dev. Ind. Pharm.* 8, 497–511.

Capece, M., 2019. The Role of Particle Surface Area and Adhesion Force in the Sticking Behavior of Pharmaceutical Powders. *J. Pharm. Sci.* 108, 3803–3813. <https://doi.org/10.1016/j.xphs.2019.08.019>

Chang, S.-Y., Sun, C.C., 2020. Interfacial bonding in formulated bilayer tablets. *Eur. J. Pharm. Biopharm.* 147, 69–75. <https://doi.org/10.1016/j.ejpb.2019.12.009>

Chattoraj, S., Daugherity, P., McDermott, T., Olsofsky, A., Roth, W.J., Tobyn, M., 2018. Sticking and Picking in Pharmaceutical Tablet Compression: An IQ Consortium Review. *J. Pharm. Sci.* 107, 2267–2282. <https://doi.org/10.1016/j.xphs.2018.04.029>

Chen, H., Paul, S., Xu, H., Wang, K., Mahanthappa, M.K., Sun, C.C., 2020. Reduction of Punch-Sticking Propensity of Celecoxib by Spherical Crystallization via Polymer Assisted Quasi-Emulsion Solvent Diffusion. *Mol. Pharm.* 17, 1387–1396. <https://doi.org/10.1021/acs.molpharmaceut.0c00086>

Danjo, K., Kojima, S., Chen, C.Y., SUNADA, H., OTSUKA, A., 1997. Effect of water content on sticking during compression. *Chem. Pharm. Bull. (Tokyo)* 45, 706–709.

de Backere, C., De Beer, T., Vervaet, C., Vanhoorne, V., 2023. Upscaling of external lubrication from a compaction simulator to a rotary tablet press. *Int. J. Pharm.* 633, 122616. <https://doi.org/10.1016/j.ijpharm.2023.122616>

Dun, J., Chen, H., Sun, C.C., 2020. Profound tabletability deterioration of microcrystalline cellulose by magnesium stearate. *Int. J. Pharm.* 590, 119927. <https://doi.org/10.1016/j.ijpharm.2020.119927>

Gunawardana, C.A., Kong, A., Wanapun, D., Blackwood, D.O., Travis Powell, C., Krzyzaniak, J.F., Thomas, M.C., Kresevic, J.E., Sun, C.C., 2023. Understanding the role of magnesium stearate in lowering punch sticking propensity of drugs during compression. *Int. J. Pharm.* 640, 123016. <https://doi.org/10.1016/j.ijpharm.2023.123016>

He, X., Secrest, P.J., Amidon, G.E., 2007. Mechanistic Study of the Effect of Roller Compaction and Lubricant on Tablet Mechanical Strength. *J. Pharm. Sci.* 96, 1342–1355. <https://doi.org/10.1002/jps.20938>

Heckel, R.W., 1961a. Density-pressure relationships in powder compaction. *Trans. Metall. Soc. AIME* 221, 671–675.

Heckel, R.W., 1961b. An analysis of powder compaction phenomena. *Trans. Metall. Soc. AIME* 221, 1001–1008.

Hooper, D., Clarke, F.C., Docherty, R., Mitchell, J.C., Snowden, M.J., 2017. Effects of crystal habit on the sticking propensity of ibuprofen—A case study. *Int. J. Pharm.* 531, 266–275. <https://doi.org/10.1016/j.ijpharm.2017.08.091>

Hutchins, A., Macdonald, B.C., Mullarney, M.P., 2012. Assessing tablet sticking propensity. *Pharm Tech* 36, 31–34.

Jahn, T., Steffens, K.-J., 2005. Press chamber coating as external lubrication for high speed rotary presses: Lubricant spray rate optimization. *Drug Dev. Ind. Pharm.* 31, 951–957. <https://doi.org/10.1080/03639040500306161>

Kakimi, K., Niwa, T., Danjo, K., 2010. Influence of compression pressure and velocity on tablet sticking. *Chem. Pharm. Bull. (Tokyo)* 58, 1565–1568.

Kottke, M.K., Rudnic, E.M., 2002. Tablet dosage forms. *Mod. Pharm.* 4, 287–330.

Li-Hua, W., Chowhan, Z.T., 1990. Drug-excipient interactions resulting from powder mixing. V. Role of sodium lauryl sulfate. *Int. J. Pharm.* 60, 61–78. [https://doi.org/10.1016/0378-5173\(90\)90190-F](https://doi.org/10.1016/0378-5173(90)90190-F)

Mitrove, A., Augsburger, L., 1980. Adhesion of tablets in a rotary tablet press I. Instrumentation and preliminary study of variables affecting adhesion. *Drug Dev. Ind. Pharm.* 6, 331–377.

Osei-Yeboah, F., Chang, S.-Y., Sun, C.C., 2016. A critical Examination of the Phenomenon of Bonding Area - Bonding Strength Interplay in Powder Tableting. *Pharm. Res.* 33, 1126–1132. <https://doi.org/10.1007/s11095-016-1858-8>

Patel, D.B., Dave, R.H., 2021. Predicting lubricants effect on tablet sticking using ketoprofen as model drug and evaluating sticking propensity using different metals and powder rheology. *Int. J. Pharm.* 606, 120913.

Paul, S., Guo, Y., Wang, C., Dun, J., Calvin Sun, C., 2023. Enabling direct compression tablet formulation of celecoxib by simultaneously eliminating punch sticking, improving manufacturability, and enhancing dissolution through co-processing with a mesoporous carrier. *Int. J. Pharm.* 641, 123041. <https://doi.org/10.1016/j.ijpharm.2023.123041>

Paul, S., Sun, C.C., 2018. Modulating Sticking Propensity of Pharmaceuticals Through Excipient Selection in a Direct Compression Tablet Formulation. *Pharm. Res.* 35, 113. <https://doi.org/10.1007/s11095-018-2396-3>

Paul, S., Sun, C.C., 2017. Lubrication with magnesium stearate increases tablet brittleness. *Powder Technol.* 309, 126–132. <https://doi.org/10.1016/j.powtec.2016.12.012>

Paul, S., Taylor, L.J., Murphy, B., Krzyzaniak, J., Dawson, N., Mullarney, M.P., Meenan, P., Sun, C.C., 2017a. Mechanism and Kinetics of Punch Sticking of Pharmaceuticals. *J. Pharm. Sci.* 106, 151–158. <https://doi.org/10.1016/j.xphs.2016.07.015>

Paul, S., Taylor, L.J., Murphy, B., Krzyzaniak, J.F., Dawson, N., Mullarney, M.P., Meenan, P., Sun, C.C., 2020. Toward a Molecular Understanding of the Impact of Crystal Size and Shape on Punch Sticking. *Mol. Pharm.* 17, 1148–1158. <https://doi.org/10.1021/acs.molpharmaceut.9b01185>

Paul, S., Taylor, L.J., Murphy, B., Krzyzaniak, J.F., Dawson, N., Mullarney, M.P., Meenan, P., Sun, C.C., 2017b. Powder properties and compaction parameters that influence punch sticking propensity of pharmaceuticals. *Int. J. Pharm.* 521, 374–383. <https://doi.org/10.1016/j.ijpharm.2017.02.053>

Paul, S., Wang, C., Wang, K., Sun, C.C., 2019. Reduced Punch Sticking Propensity of Acesulfame by Salt Formation: Role of Crystal Mechanical Property and Surface

Chemistry. Mol. Pharm. 16, 2700–2707.
<https://doi.org/10.1021/acs.molpharmaceut.9b00247>

Roberts, M., Ford, J.L., MacLeod, G.S., Fell, J.T., Smith, G.W., Rowe, P.H., 2003. Effects of surface roughness and chrome plating of punch tips on the sticking tendencies of model ibuprofen formulations. *J. Pharm. Pharmacol.* 55, 1223–1228.

Roberts, M., Ford, J.L., MacLeod, G.S., Fell, J.T., Smith, G.W., Rowe, P.H., Dyas, A.M., 2004. Effect of punch tip geometry and embossment on the punch tip adherence of a model ibuprofen formulation. *J. Pharm. Pharmacol.* 56, 947–950.

Sun, C.C., 2017. Microstructure of Tablet—Pharmaceutical Significance, Assessment, and Engineering. *Pharm. Res.* 34, 918–928. <https://doi.org/10.1007/s11095-016-1989-y>

Sun, C.C., 2015. Dependence of ejection force on tableting speed—A compaction simulation study. *Powder Technol.* 279, 123–126. <https://doi.org/10.1016/j.powtec.2015.04.004>

Sun, C.C., 2011. Decoding Powder Tabletability: Roles of Particle Adhesion and Plasticity. *J. Adhes. Sci. Technol.* 25, 483–499. <https://doi.org/10.1163/016942410X525678>

Swaminathan, S., Ramey, B., Hilden, J., Wassgren, C., 2017. Characterizing the powder punch-face adhesive interaction during the unloading phase of powder compaction. *Powder Technol.* 315, 410–421.

Uzunović, A., Vranić, E., 2007. Effect of magnesium stearate concentration on dissolution properties of ranitidine hydrochloride coated tablets. *Bosn. J. Basic Med. Sci.* 7, 279.

Vreeman, G., Sun, C.C., 2022. A powder tabletability equation. *Powder Technol.* 408, 117709. <https://doi.org/10.1016/j.powtec.2022.117709>

Waimer, F., Krumme, M., Danz, P., Tenter, U., Schmidt, P.C., 1999. The influence of engravings on the sticking of tablets. Investigations with an instrumented upper punch. *Pharm. Dev. Technol.* 4, 369–375.

Waknis, V., Chu, E., Schlam, R., Sidorenko, A., Badawy, S., Yin, S., Narang, A.S., 2014. Molecular Basis of Crystal Morphology-Dependent Adhesion Behavior of Mefenamic Acid During Tableting. *Pharm. Res.* 31, 160–172. <https://doi.org/10.1007/s11095-013-1149-6>

Wang, C., Paul, S., Sun, D.J., Nilsson Lill, S.O., Sun, C.C., 2020. Mitigating Punch Sticking Propensity of Celecoxib by Cocrystallization: An Integrated Computational and Experimental Approach. *Cryst. Growth Des.* 20, 4217–4223. <https://doi.org/10.1021/acs.cgd.0c00492>

Wang, J.J., Guillot, M.A., Bateman, S.D., Morris, K.R., 2004. Modeling of adhesion in tablet compression. II. Compaction studies using a compaction simulator and an instrumented tablet press. *J. Pharm. Sci.* 93, 407–417. <https://doi.org/10.1002/jps.10553>

Wang, Z., Shah, U.V., Olusanmi, D., Narang, A.S., Hussain, M.A., Gamble, J.F., Tobyn, M.J., Heng, J.Y.Y., 2015. Measuring the sticking of mefenamic acid powders on stainless steel surface. *Int. J. Pharm.* 496, 407–413. <https://doi.org/10.1016/j.ijpharm.2015.09.067>